

RESEARCH

Open Access



TRPV4 modulates inflammatory responses and apoptosis in enteric glial cells triggered by *Clostridioides difficile* toxins A and B

Dvison de Melo Pacífico^{1†}, Deiziane Viana da Silva Costa^{2†}, Maria Lucianny Lima Barbosa¹, Conceição Silva Martins Rebouças¹, Simone de Goes Simonato¹, Cirle Alcantara Warren², Maria Luana Gaudencio dos Santos Morais¹, Renata Ferreira de Carvalho Leitao^{1*} and Gerly Anne de Castro Brito¹

Abstract

Clostridioides difficile, a spore-forming anaerobic bacterium, is the primary cause of hospital antibiotic-associated diarrhea. Key virulence factors, toxins A (TcdA) and B (TcdB), significantly contribute to *C. difficile* infection (CDI). Yet, the specific impact of these toxins, particularly on enteric glial cells (EGCs), still needs to be fully understood. This study examines the role of the transient receptor potential vanilloid 4 (TRPV4), a calcium-permeable channel, in the inflammatory response and apoptosis of EGCs induced by TcdA and TcdB and evaluates TRPV4 expression in the cecum and colon of infected mice. EGCs were treated with TcdA (50ng/mL) or TcdB (1ng/mL) for 18 h, with or without the TRPV4 antagonist RN-1734 (100 μM), to assess TRPV4 gene and protein levels, inflammatory markers, and cell death. *C. difficile* infected mice were euthanized on day 3 post-infection for TRPV4 expression in the cecum and colon. Findings reveal that EGCs naturally express TRPV4, increasing its expression by TcdA and TcdB exposure. CDI significantly upregulates TRPV4 in the cecum and colon's submucosal and myenteric plexus regions. TRPV4 mediates TNF-α release in EGCs and is partially involved in the increase in *IL-6* gene expression triggered by these toxins. Our results highlight TRPV4's role in triggering EGC apoptosis via caspase 3 activation and inhibiting the reduction of Bcl-2, an anti-apoptotic protein in EGCs caused by *C. difficile* toxins. These results highlight TRPV4's significant role in CDI pathogenesis and its potential as a therapeutic target to counteract the detrimental effects of *C. difficile* toxins on enteric glia.

Keywords *C. difficile*, Enteric glia, TRPV4, Inflammation, Cell death

[†]Dvison de Melo Pacífico and Deiziane Viana da Silva Costa contributed equally to this work.

*Correspondence:

Renata Ferreira de Carvalho Leitao
renata.carvalho@ufc.br

¹Department of Morphology, Faculty of Medicine, Federal University of Ceará, Fortaleza, CE, Brazil

²Division of Infectious Diseases and International Health, University of Virginia, Charlottesville, Virginia, VA, USA



© The Author(s) 2024. **Open Access** This article is licensed under a Creative Commons Attribution-NonCommercial-NoDerivatives 4.0 International License, which permits any non-commercial use, sharing, distribution and reproduction in any medium or format, as long as you give appropriate credit to the original author(s) and the source, provide a link to the Creative Commons licence, and indicate if you modified the licensed material. You do not have permission under this licence to share adapted material derived from this article or parts of it. The images or other third party material in this article are included in the article's Creative Commons licence, unless indicated otherwise in a credit line to the material. If material is not included in the article's Creative Commons licence and your intended use is not permitted by statutory regulation or exceeds the permitted use, you will need to obtain permission directly from the copyright holder. To view a copy of this licence, visit <http://creativecommons.org/licenses/by-nc-nd/4.0/>.

Introduction

Clostridioides difficile (*C. difficile*), a Gram-positive, spore-forming anaerobic bacterium found in the human gastrointestinal tract, has emerged as a significant enteropathogen, largely attributed to its association with antibiotic use, which disrupts the natural microbial balance [1, 2]. This bacterium produces a range of proteins critical to its pathogenicity. Among these, *C. difficile* toxins A (TcdA) and B (TcdB) are particularly noteworthy as the primary virulence factors, directly contributing to the clinical symptoms and outcomes of *C. difficile* infection (CDI) [3].

The cytotoxic effects of *C. difficile* toxins allow the pathogen to infiltrate the deeper layers of the intestinal mucosa, impacting not only the intestinal mucosal cells but also cells within other layers of the intestine [4]. Specifically, enterocytes, colonocytes, and enteric neurons are particularly vulnerable to the cytotoxic impacts of TcdA and TcdB, leading to a wide range of clinical manifestations seen in CDI [5–7]. Recent research, including studies from our group, has demonstrated the role of enteric glial cells (EGCs) in the pathophysiology of CDI [8–10].

EGCs, specialized non-neuronal glial cells within the enteric neuron system (ENS), are distributed throughout the intestinal tract [11]. As integral components of the ENS, EGCs play crucial roles in maintaining the normal function of the intestinal tract under physiological conditions, regulating gut motility, intestinal barrier integrity, and the modulation of immune responses. Beyond their established roles in normal physiological processes, EGCs have also been documented in the literature as playing critical roles in various intestinal pathophysiological conditions, including Crohn's disease, ulcerative colitis, irritable bowel syndrome, and CDI [12,13]. The pivotal role of these cells in gastrointestinal disorders underscores their substantial contributions to gut health and their involvement in inflammatory responses through dynamic interactions with other cell types in the complex gut environment [11]. However, the precise mechanisms by which these cells impact such processes still need to be fully understood. This area of research has been relatively overlooked within the scientific community, particularly compared to the extensive research focused on other gut cell types, such as epithelial cells. Our study aims to address this gap by spotlighting the effects of *C. difficile* toxins on EGCs.

The transient receptor potential vanilloid 4 (TRPV4) is among the most extensively studied members of the transient receptor potential (TRP) ion channels superfamily. It functions as a polymodal cation channel with high permeability to Ca²⁺, activated by various physical and chemical stimuli such as heat, cellular swelling, and endogenous ligands, including arachidonic acid and its

metabolites [14–17]. TRPV4 expression has been identified in the myenteric plexus of the human colon and immune system cells, such as macrophages, neutrophils, and dendritic cells [16–18]. Moreover, TRPV4 shows widespread expression in the stomach, small intestine, and colon within the intestinal tract of rodents [19].

The association of TRPV4 with the pathophysiology of inflammatory bowel disease (IBD) [20] underscores its significance in intestinal inflammation research, spotlighting its potential contribution to the mechanisms driving intestinal disorders. Despite its established involvement in IBD, a condition closely associated with an increased risk of CDI, the specific role of TRPV4 in the pathophysiology of CDI remains unexplored in current scientific literature.

For the first time, this research explores whether EGCs express TRPV4 under physiological conditions and during CDI. Furthermore, it aimed to investigate the role of this receptor in modulating the inflammatory response and cell death induced by *C. difficile* toxins in EGCs.

Methods

In vivo studies

Mice

Male C57BL/6 mice, 8 weeks old, were obtained from the Jackson Laboratory, Farmington, US. Furthermore, these animals were accommodated in polypropylene cages lined with wood shavings, with bedding changes occurring twice a week. Throughout the experiments, the animals were maintained in consistent environmental conditions (temperature: 22°C ± 2°C, with air exhaustion, and a 12 h light/12 h dark cycle). They had unrestricted access to water and standard chow diet ad libitum.

We confirm that all experimental protocols conducted in this study were approved by the Ethics of Animal Experiments Committee at the University of Virginia (Protocol number 4096). Additionally, we affirm that the reporting of all methods in this study aligns with the Animal Research: Reporting of In Vivo Experiments (ARRIVE) guidelines, ensuring transparency and rigor in presenting our findings.

C. difficile infection model

The murine CDI model utilized in this study follows a well-established protocol due to its ability to mimic clinical symptoms, such as severe diarrhea, presented by humans with CDI [8]. This model consists of disturbing the animal's microbiota and thus facilitating colonization or infection by *C. difficile* in wild-type (WT) C57BL/6 mice ($n=6$ for each group). The animals received a cocktail of antibiotics in their drinking water for 3 days, consisting of 0.035 mg per mL of gentamicin, 850 U per mL of colistin, 0.215 mg per mL of metronidazole, and 0.045 mg per mL of vancomycin, as illustrated in Fig. 1.

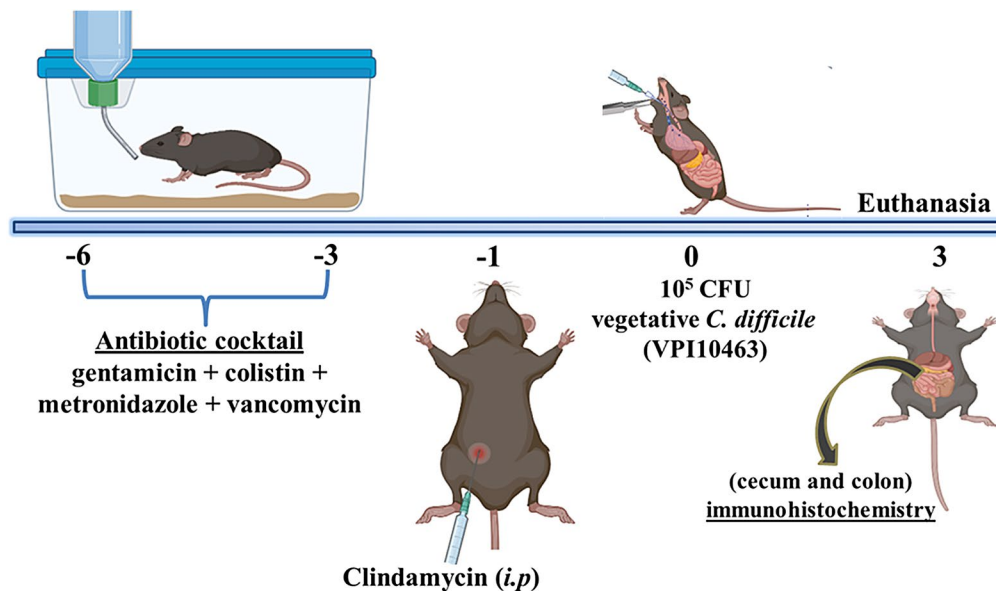


Fig. 1 *C. difficile* infection model induction scheme

Following a 2-day antibiotic-free period, the animals received an intraperitoneal injection of clindamycin (32 mg per kg, i.p.) 1 day before *C. difficile* challenge. Subsequently, 10^5 CFU (in 100 μ L of chopped meat broth, a pre-reduced medium) of the vegetative *C. difficile* strain VPI10463 (ATCC 43255, *tcdA* + *tcdB* + *cdtB*-) was administered by oral gavage. Control mice received chopped meat broth (100 μ L). The mice's weight and disease symptoms development were monitored daily. Three days after infection, animals were euthanized using a combination of ketamine (180 mg/kg; i.p.) and xylazine (15 mg/kg, i.p.). Segments from the cecum and colon were collected and processed for immunohistochemistry analysis.

Immunohistochemistry

Section (4 μ m thick) were prepared from paraffin-embedded mouse cecum and colon tissues. After deparaffinization, antigens were recovered by incubating the slides in citrate buffer (pH 9.0) for 20 min at 95 $^{\circ}$ C in a PT link tank (DAKO). To reduce non-specific binding, endogenous peroxidase was blocked with 3% H_2O_2 for 10 min. The sections were then incubated overnight with an Anti-TRPV4 antibody (ab39260, Abcam, 1:1000), followed by a 30-minute incubation with polymer HRP (K8000, Dako). The antibody-binding sites were visualized by incubating the samples with diaminobenzidine- H_2O_2 (DAB, Dako) solution. The brown coloration indicates positive staining. The number of immunopositive cells was quantified using ImageJ software by counting cells with positive staining in ten distinct fields per slide, focusing on the "hot areas" (regions with intense staining). This analysis used one slide per animal and four specimens per group [21].

In vitro studies

Rat EGC culture and treatment

The immortalized EGC line used in this study comes from the jejunum region of *Rattus norvegicus* ATCC (PK060399egfr CRL-2690, Virginia-United States). These cells have demonstrated morphological and functional characteristics comparable to primary EGCs [22].

EGCs were cultured in DMEM medium (Dulbecco's Modified Eagle's Medium, Gibco) and supplemented with 10% fetal bovine serum, 1% antibiotics (100 mg/mL penicillin and 100 mg/mL streptomycin, Gibco), and 1 mM sodium pyruvate (Gibco) at 37 $^{\circ}$ C in a humidified incubator under 5% CO_2 for no more than 25 passages. For all experiments in this research, EGCs were released from the culture flasks using 0.05% trypsin-EDTA for 5 min. The cells were incubated with the TRPV4-specific antagonist (RN-1734-100 μ M, Cayman, 946387-07-1) for 1 h before incubation with TcdA (50 ng/mL) or TcdB (1 ng/mL). In an additional experiment, we included a group of cells exposed simultaneously to both toxins. We maintained the same exposure time and concentrations evaluated in individual toxin treatments, with or without the TRPV4 antagonist. The concentration of RN-1734 was obtained from the results of the MTT assay (Fig. S1 – supplementary material). Furthermore, it is worth highlighting that TcdA and TcdB used in the study were purified from TechLab (Virginia-United States), and these, in turn, were produced by the *C. difficile* strain VPI10463.

Quantitative real-time PCR (qPCR)

Initially, we aimed to determine whether EGCs express the TRPV4 receptor, establishing this as a prerequisite

for advancing our research. To achieve this objective, we investigated the gene expression of TRPV4 by the Polymerase Chain Reaction (PCR) at 2, 12, and 18 h following incubation with either TcdA or TcdB. Subsequently, our research extended to examine other genes that may play a role in the pathophysiology of CDI, such as *interleukin-6* (*IL-6*), interleukin-1 beta (*IL-1-β IL-1β*), and antiapoptotic *B-cell lymphoma family gene 2* (*bcl-2*) genes, using *glyceraldehyde-3-phosphate dehydrogenase* (*GAPDH*) as the reference gene.

EGCs (6×10^5 cells/well), at passage 20, were cultivated in 6-well plates and incubated with TcdA (50ng/mL) or TcdB (1ng/mL) for 18 h. The control group of cells was cultured exclusively in a culture medium (DMEM) without exposure to *C. difficile* toxins (control). After incubation, total RNA extraction was performed using a RNeasy Plus Mini Kit (Qiagen, Hilden, Germany) on the QIAcube platform (Qiagen). Furthermore, RNA was quantified using the equipment Nanodrop. The RNA's purity was evaluated using the following proportions: nucleic acids/proteins (260/280) and nucleic acids/other contaminants (260/230). Then, the RNA underwent reverse transcription using a High-Capacity cDNA Reverse Transcription Kit (Thermo Fisher Scientific) according to the manufacturer's protocol.

Amplification of *TRPV4*, *GAPDH*, *IL-6*, *IL-1-β*, and *bcl-2* genes in cell samples was carried out using the StepOne apparatus. Amplification of specified genes in EGC samples was performed using a CFX Connect system (Bio-Rad) with the following conditions: 95 °C for 30 s, 40 cycles of 95 °C for 5 s, and 60 °C for 30 s, and analysis of the melting curve from 65 to 95 °C in increments of 0.5 °C for 2 s each. Gene expression was calculated by the Livak & Schmittgen method ($2^{-\Delta\Delta Ct}$).

Following the same procedural steps described, the cells were co-incubated for 18 h with either TcdA or TcdB and the TRPV4 pharmacological modulator (RN-1734). We have also analyzed and compared the protein and gene expression profiles when cells were pre-treated with the TRPV4 modulator for one hour before toxin exposure. The primer sets used for these experiments are listed in Supplementary Material (Table S1).

Western blotting analysis

To assess the expression of TRPV4 protein, EGCs (6×10^5 cells/well) were seeded into 6-well plates and subsequently incubated with TcdA or TcdB for 18 h.

Following incubation, the supernatant was discarded, and the cells were lysed with RIPA lysis buffer (Thermo Fisher Scientific, containing EDTA and phosphatase-free protease inhibitor). The lysate was centrifuged for 17 min at 4 °C and 15.773 g, and the supernatant was collected for further analysis.

Protein concentrations were determined using the bicinchoninic acid assay following the manufacturer's instructions (Thermo Fisher Scientific). Forty micrograms of protein, previously mixed with Laemmli sample buffer and β-mercaptoethanol, were denatured at 95 °C for 5 min. Subsequently, these proteins were separated on 10% BIS-Tris gel and transferred onto PVDF membranes for 2 h.

Following the transfer, the membranes were blocked with a 5% blocking solution (BioRad) at room temperature for 1 h. They were then incubated overnight at 4 °C with primary antibodies (anti-α-tubulin 1:500, Sigma-Aldrich T8203 and anti-TRPV4 1:2000, abcam39260). After primary antibody incubation, membranes were exposed to secondary antibodies (anti-mouse 1:500 and anti-rabbit 1:500) for 1 h and 30 min. Membranes were washed in Tris-buffered saline containing 0.05% Tween 20 (TSB-T) and then incubated with Enhanced Chemiluminescence – ECL (Biorad 1705060). The chemiluminescence signal was detected using a ChemiDoc system (BioRad). Densitometric quantification of bands was performed using ImageLab software (BioRad).

In a distinct experimental set, replicating all the previously described procedural steps, the protein expression of cleaved caspase-3 (an apoptosis marker) was assessed in EGCs exposed to TcdA and TcdB in the presence or absence of the TRPV4 antagonist. Specifically, cells were pretreated with RN-1734 (100μM) 1 h before toxin incubation. The antibodies used included primary antibodies (β-actin 1:200, Santa Cruz sc-7210; cleaved Caspase-3, 1:400, Millipore AB3623) and the secondary antibody (anti-rabbit; 1:400).

We used the ImageJ software to quantify Western blot bands. After selecting each band of interest by drawing a rectangular box around it, ensuring the band was fully encompassed, the software generated a peak for each band. The area under the curve of each peak corresponded to the band's intensity. The signal intensity, expressed in pixels, was directly proportional to the target protein concentration. To account for any variations in sample loading, the intensity of each target band was normalized by dividing it by the intensity of the corresponding loading control band. This normalization step ensured standardized data and allowed for reliable comparisons between samples.

Immunofluorescence

Immunofluorescence was performed to investigate the localization of the TRPV4 receptor in EGCs following an 18-hour treatment with TcdA or TcdB. EGCs at passage 17 were seeded in 24-well plates (4×10^4 cells/well). After the 18 h incubation period with the toxins, the cells were fixed in 4% paraformaldehyde (500 μL per well) for 15 min, followed by permeabilization in PBS containing

0.025% Triton X100 (Sigma-Aldrich) and 0.2% bovine serum albumin (BSA, Sigma-Aldrich) for 15 min. After permeabilization, cells were blocked with 0.25% Triton X100 (Sigma-Aldrich) and 5% BSA (Sigma-Aldrich) in PBS at room temperature for 1 h, then washed with a washing solution. Then, the cells were incubated with an anti-TRPV4 primary antibody (1:1000, abcam39260) or cleaved Caspase-3 (1:400, Millipore AB3623) at 4°C overnight. After three washes with wash buffer (0.01% Tween 20 in PBS), cells were overnight incubated with Alexa-Fluo 488 secondary antibody (1:400, Invitrogen). Following a wash with PBS, cells were mounted with ProLong Gold antifade reagent containing DAPI (Thermo Scientific, P36931). The samples were visualized by confocal fluorescence microscopy (LM10-Confocal Zeiss).

Immunofluorescence for TRPV4 or cleaved Caspase-3 was assessed using ten digital images captured in each section, with four samples per group. The average positive fluorescence intensity was quantified using Zeiss software. The average fluorescence intensity was quantified using Zeiss software. The software allows the selection of specific channels, such as DAPI and the protein of interest. In this case, the green channel, corresponding to the protein of interest, was selected. After completing the analysis, the software generated a table displaying the arithmetic mean intensity, representing the fluorescence intensity for the selected protein.

In a separate experimental set, to assess the impact of blocking TRPV4 with RN-1734) on the nuclear translocation of the transcription factor NFκBp65 in EGCs, as well as its effect on the expression of TNF-α, cells were pre-incubated with RN-1734 1 h before to exposure to TcdA or TcdB. The primary antibodies used were anti-NFκBp65 (1:500, Abcam 16502) and anti-TNF-α (1:500, Abcam 6671), along with the secondary antibody (Alexa Fluor 488, 1:400, Invitrogen). The remaining steps of the procedure were carried out as previously described, with an average of 10 images acquired per slide. The average TNF-positive fluorescence intensity was quantified using Zeiss software. The percentage of NFκB p65-positive cells was determined by counting 100 cells per coverslip across five separate experiments, focusing on the “hot areas” (regions exhibiting intense staining).

To evaluate the effect of TRPV4 activation by its agonist, GSK 1,016,790 A (50 nM/ml), and inhibition by its antagonist, RN-1734 (100 μM), on caspase-3 activation in EGCs, cells were pre-incubated with either GSK 1,016,790 A or RN-1734 for 1 h before exposure to TcdA or TcdB. The primary antibody was anti-cleaved Caspase-3 (1:400, Millipore AB3623), followed by the secondary antibody Alexa Fluor 488 (1:400, Invitrogen). The remaining steps were conducted as previously described, with an average of 10 images acquired per slide. The cleavage caspase-3-positive fluorescence intensity was

quantified using Zeiss software following the procedure described above.

Realtime-glo annexin V apoptosis assay

Cell death was assessed using a live cell real-time assay (Realtime-Glo annexin V apoptosis assay, Promega, JA1000), following the manufacturer’s instructions. EGCs (10^4 cells/well), at passage 20, were seeded in white tissue culture-treated 96-well plates (Falcon, solid white bottom). These cells were incubated with TcdA, TcdB or both TcdA and TcdB simultaneously for 18 h, in either the absence or presence of RN-1734, added 1 h before exposure to the *C. difficile* toxins. Subsequently, 200 μL of 2x detection reagent (containing 2 μL of annexin NanoBit substrate, 2 μL of CaCl₂, 2 μL of annexin V-SmBit, and 2 μL of annexin V-LgBit in 1000 μL of pre-warmed, supplemented DMEM) was added to each well. The cells were then incubated at 37 °C in a humidified incubator under 5% CO₂. Luminescence readings were recorded using a luminometer (NanoLuc technology ready, Promega). The intrinsic luminescence of the reagent (no-cell, no-compound background control) was subtracted from the sample luminescence signals. The adjusted values were normalized against the mean of control cells to obtain the relative luminescent units (RLUs).

Assessment of intracellular calcium levels

To assess intracellular Ca²⁺ levels, EGCs were seeded at a density of 60,000 cells per well in black 96-well plates. The intracellular Ca²⁺ levels were measured using the Fluo-8 no wash calcium assay kit (Abcam, ab112129) following the manufacturer’s instructions. In brief, 100 μL of Fluo-8 dye-loading solution was added to each well and incubated at 37 °C for 30 min. This was followed by an additional 30-minute incubation at room temperature to ensure optimal dye uptake. Afterward, the cells were treated with TcdA and TcdB, and/or the TRPV4 antagonist, with the antagonist being added one hour prior to toxin incubation. Fluorescence intensity was monitored at an excitation/emission wavelength of 490/525 nm at different time points using the Infinite 200 PRO-Tecan plate reader. The fluorescence intensity of Fluo-8 (Ex/Em=490/525) directly corresponds to the increase in intracellular calcium levels.

Statistical analysis

All quantitative results obtained in this research were expressed as mean ± standard error of the mean (SEM). Statistical analysis of the data was performed using *GraphPad Prism* software, version 8.0. The student’s t-test was used to compare the means between two groups, and the analysis of variance (ANOVA) followed by Tukey’s test was used to compare the means among

three or more groups. A p-value ≤ 0.05 was considered statistically significant.

Results

***C. difficile* infection increases TRPV4 expression in the cecum and colon of mice**

TRPV4 is naturally expressed in the cecum and colon's mucosa immune cells (orange arrows) and myenteric plexus regions (red arrow) of healthy mice (control) (Fig. 2A). Following CDI, there was a marked elevation in the expression of this receptor across both the cecum and colon. Notably, an increase in TRPV4 immunostaining was observed in the epithelial, submucosal, and myenteric plexus cells of infected mice (red arrow) compared to the control group, which was not infected.

Furthermore, increased immunostaining in immune cells (yellow arrows) can also be observed in infected animals.

Figure 2B shows that the number of TRPV4-positive cells in the CDI group within the cecum and colon is significantly increased compared to the control group (uninfected mice). This evidence further supports the involvement of this receptor in the context of infection, highlighting its potential role in mediating the immune response to CDI.

TcdA and TcdB upregulation the TRPV4 gene and protein expression in EGCs

We found that EGCs constitutively express the TRPV4 receptor and that exposure to TcdA and TcdB led to a gradual increase in basal TRPV4 gene expression over time (Fig. 3A). In addition, both toxins significantly

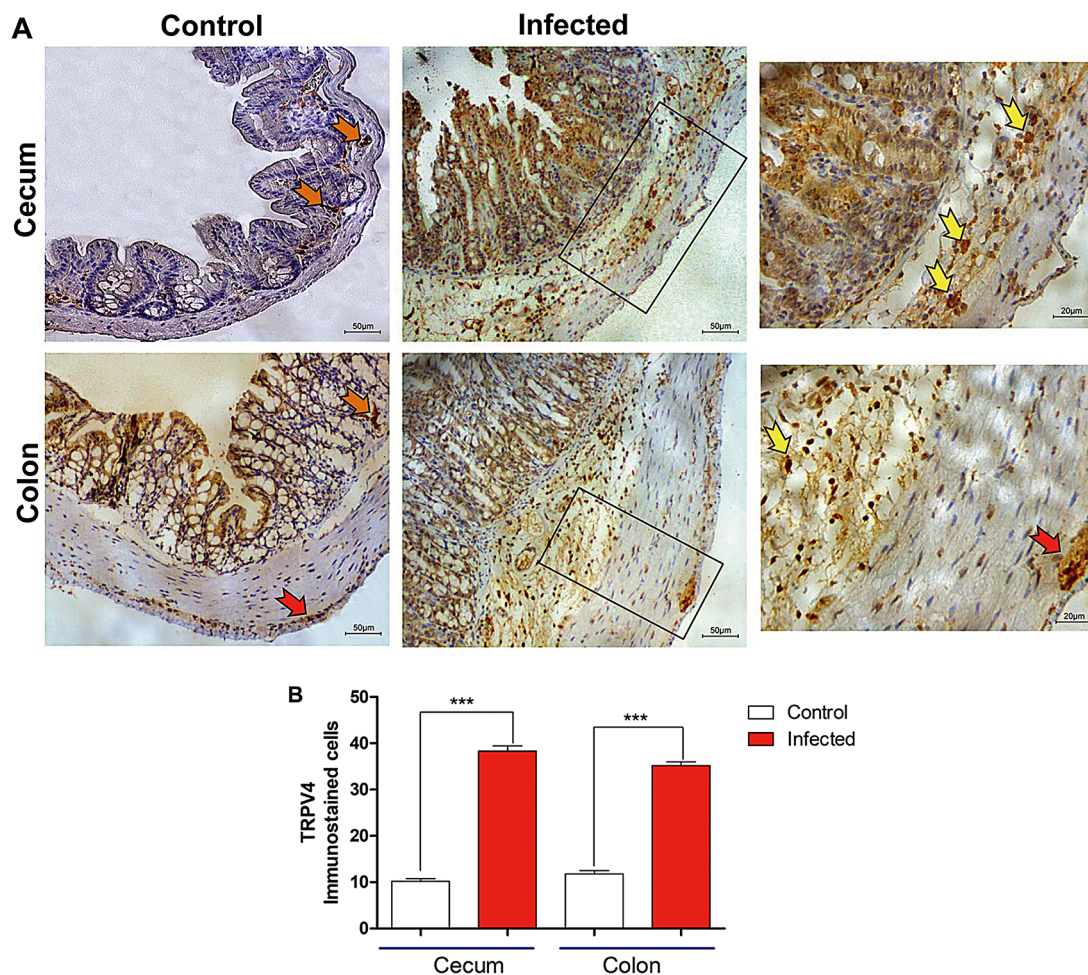


Fig. 2 *C. difficile* infection (CDI) increases the expression of TRPV4 in the cecum and colon of infected mice. **A)** Photomicrographs showing the immunohistochemical staining for TRPV4 within the intestinal regions (cecum and colon) of uninfected mice and those subjected to CDI. In the control group (uninfected animals), TRPV4 is constitutively expressed in the mucosa immune cells (orange arrow) and myenteric plexus (red arrow); in animals exposed to *C. difficile*, a pronounced increase in immunostaining is observed in the cecum and colon, particularly in immune cells (yellow arrows) and in the myenteric plexus (red arrow), clearly observed at 400x magnification (Scale bar = 20 μ m). The standard images were taken at 100x magnification (Scale bar = 50 μ m). **B)** The graph represents the mean \pm SEM of the number of immunopositive cells for TRPV4 in the cecum and colon of mice subjected to CDI (infected group) and non-infected (control group). Statistical analysis was conducted using the student's t-test was used. *** $p < 0.0001$

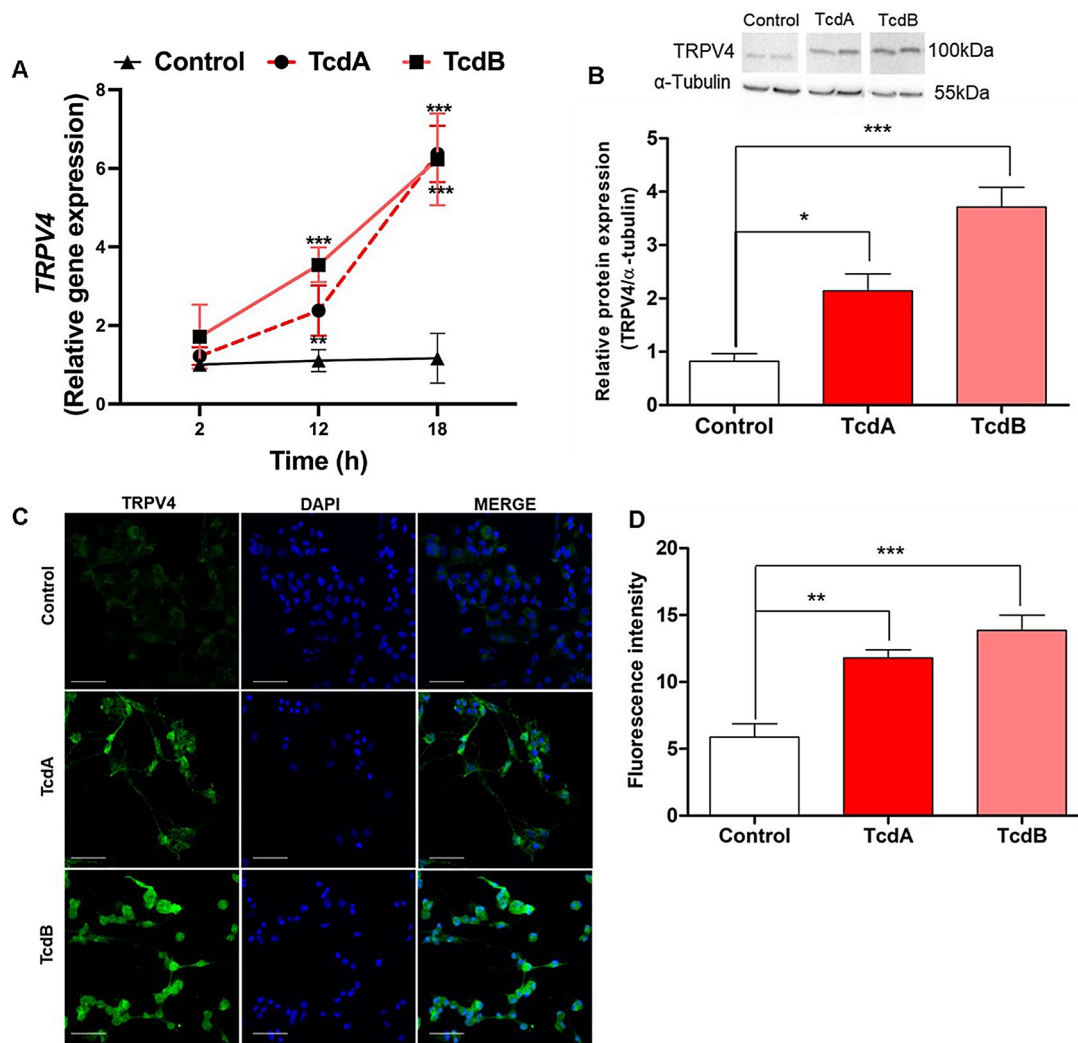


Fig. 3 *C. difficile* toxins A (TcdA) and B (TcdB) increase TRPV4 gene and protein expression in enteric glial cells (EGCs) in vitro. **A**) Administration of TcdA (50ng/mL) and TcdB (1ng/mL) led to a significant elevation in TRPV4 gene expression in EGCs. The gene expression was evaluated by qPCR after incubating EGCs with the toxins for 2, 12 and 18 h. The data are presented as mean \pm SD of the relative expression of TRPV4. Statistical significance was determined using the two-way ANOVA and Tukey tests; ** $p < 0.006$ and *** $p < 0.0001$. **B**) TcdA and TcdB significantly increase TRPV4 protein expression in EGCs, assessed by Western Blotting. Data are presented as mean \pm SEM, normalized to α -tubulin for comparison. Statistical significance was determined using the one-way ANOVA and Tukey tests. * $p < 0.001$ and *** $p < 0.0001$. **C**) Exposure to TcdA and TcdB increases the cytoplasmic immunostaining of TRPV4 in EGCs. Photomicrographs showcase the cytoplasmic immunostaining of TRPV4 (green), the nuclear staining with DAPI (blue), and the merged images (MERGE). **D**) illustrate the quantification of the mean fluorescence intensity of TRPV4 immunostaining in EGCs, measured using Zeiss software. The results are expressed as mean \pm SEM of TRPV4 immunostaining fluorescence intensity. Statistical significance was determined using the one-way ANOVA and Tukey tests. * $p < 0.001$ and *** $p < 0.0001$. The entire blotting membranes are available in the supplementary material (Figures S2 and S3)

increased the TRPV4 protein expression in EGCs detected by Western Blot over the 18-hour incubation period compared to the control group (Fig. 3B).

Figure 3C supports the Western Blot findings by illustrating the cytoplasmic immunostaining of the TRPV4 receptor in EGCs (green). Notably, upon exposure to TcdA and TcdB, there was a noticeable increase in the immunostaining of this receptor in EGCs compared to the control group. Consistent with these qualitative observations (Fig. 3C), the quantification of the fluorescence intensity of TRPV4 immunostaining revealed

that TcdA and TcdB significantly increased TRPV4 protein expression in EGCs compared to the control group (Fig. 3D).

Blocking TRPV4 by RN-1734 reduces translocation of NF κ Bp65 in EGCs by TcdA and TcdB

To assess the involvement of TRPV4 in activating the NF κ B transcription factor in EGCs upon exposure to TcdA and TcdB, we examined the nuclear expression of NF κ Bp65 using immunofluorescence in EGCs exposed to TcdA and TcdB in the presence of a TRPV4 inhibitor.

Our results indicate that TcdA and TcdB significantly increased the number of NFκBp65 positive cells compared to the control group cultured exclusively in DMEM (Fig. 4A). This finding suggests that TcdA and TcdB directly contribute to the activation of NFκB. In contrast, pre-treating EGCs with RN-1734, a TRPV4 inhibitor, one hour before exposure to TcdA or TcdB partially prevented the nuclear translocation of NFκBp65 (Fig. 4A), indicating that TcdA and TcdB activate NFκB through TRPV4. Furthermore, there were no significant differences between the control group and the RN-1734-treated group of cells, which were incubated with the TRPV4 antagonist but not exposed to TcdA or TcdB, indicating that RN-1734's effect is specific to the condition of toxin exposure.

The expression of NFκBp65 is visualized by immunolabelling in Fig. 4B.

Blocking TRPV4 by RN-1734 reduces the inflammatory response in EGCs triggered by TcdA and TcdB

Building on our research group's prior findings, which highlighted the impact of TcdA and TcdB on EGCs [8, 9], leading to the secretion of inflammatory cytokines, we aimed to elucidate the role of the TRPV4 receptor in this process. Specifically, we investigated whether blocking the TRPV4 receptor with its antagonist, RN-1734 could decrease the gene expression of *IL-6* and *IL-1β* and the protein expression of TNF-α in EGCs exposed to TcdA and TcdB.

Our findings show that inhibiting TRPV4 with RN-1734 significantly reduces *IL-6* gene expression in EGCs exposed to TcdA. In contrast, this effect was not evident in cells subjected to TcdB treatment (Fig. 5A). Additionally, we observed that TcdA and TcdB increased *IL-1β* gene expression (Fig. 5B) and TNF-α protein expression (Fig. 5C) in EGCs compared to the control group. However, the impact of the *C. difficile* toxins on *IL-1β* expression seems to be TRPV4-independent, as inhibiting this receptor with RN-1734 failed to prevent the increased *IL-1β* gene expression induced by the toxins (Fig. 5B). On the contrary, RN-1734 reduced TNF protein expression induced by TcdA and TcdB (Fig. 5C), suggesting that TRPV4 plays a role in this process.

The expression of TNF in EGCs is visualized by immunolabelling in Fig. 5D.

Blocking TRPV4 reduces toxins-induced cell death in EGCs by reducing caspase-3 and upregulating *bcl-2* expression

To investigate the impact of the TRPV4 receptor on apoptosis induced by *C. difficile* toxins, we utilized the real-time Glo-annexin V apoptosis assay. Furthermore, we analyzed the expression of activated caspase-3 protein and *bcl-2* gene expression, which serve as indicators of cell survival.

In Fig. 6A, we observe a significant increase in the death of EGCs when exposed to TcdA and TcdB compared to the control groups. Both toxins prompted an increase in the formation of the apoptotic conjugate, evidenced by the binding of annexin V to phosphatidylserine on the outer layer of the cell membrane. Conversely, the inhibition of TRPV4 with RN-1734 significantly reduced the death of EGCs triggered by TcdA and TcdB.

The effect of TcdA and TcdB in promoting apoptosis in EGCs was confirmed, as exposure to these toxins resulted in a significant increase in caspase-3 protein expression compared to the control group. This effect appears to be dependent on the TRPV4 receptor, as the inhibition of this receptor with its antagonist substantially reduced the expression of caspase-3 protein in EGCs exposed to TcdA or TcdB (Fig. 6B).

Furthermore, TcdA and TcdB decrease the gene expression of *bcl-2* in EGCs compared to the control group, reducing cell survival. RN-1734 blocks the TRPV4 receptor, protecting the cells from this toxic effect. We observed an upregulation of *bcl-2* gene expression in EGCs pre-incubated with RN-1734 and subsequently exposed to TcdA or TcdB (Fig. 6C).

Given that TcdA and TcdB are released concomitantly in vivo to promote disease, we next investigated whether the TRPV4 antagonist could protect EGCs simultaneously exposed to both toxins (TcdA and TcdB). TRPV4 blockade effectively reduced EGCs death induced by *C. difficile* toxins. Interestingly, there was no difference in cell death between cells exposed to TcdA or TcdB alone compared to those exposed to both toxins combined (Fig. 6D).

These findings indicate that activating the TRPV4 receptor in EGCs modulates the apoptotic effects of *C. difficile* toxins. Moreover, inhibiting TRPV4 with its antagonist significantly reduces toxin-induced enteric glia apoptosis, highlighting its critical role in protecting these cells from toxic effects.

TRPV4 activation promotes EGC death via Caspase-3 activation (cleavage), while TRPV4 inhibition attenuates toxin-induced apoptosis

To confirm the role of TRPV4 in enteric glial cell (EGC) death, we incubated these cells with the TRPV4 agonist GSK1016790A and assessed its effect on activated caspase-3 expression. Compared to control groups, a significant increase in activated caspase-3 protein was observed in EGCs treated with GSK1016790A. Likewise, exposure to TcdA and TcdB led to a marked activation of caspase-3 compared to controls. This increase in cleaved caspase-3 induced by *C. difficile* toxins appears to be TRPV4-dependent, as treatment with the TRPV4 antagonist significantly reduced caspase-3 cleavage in EGCs exposed to either TcdA or TcdB.

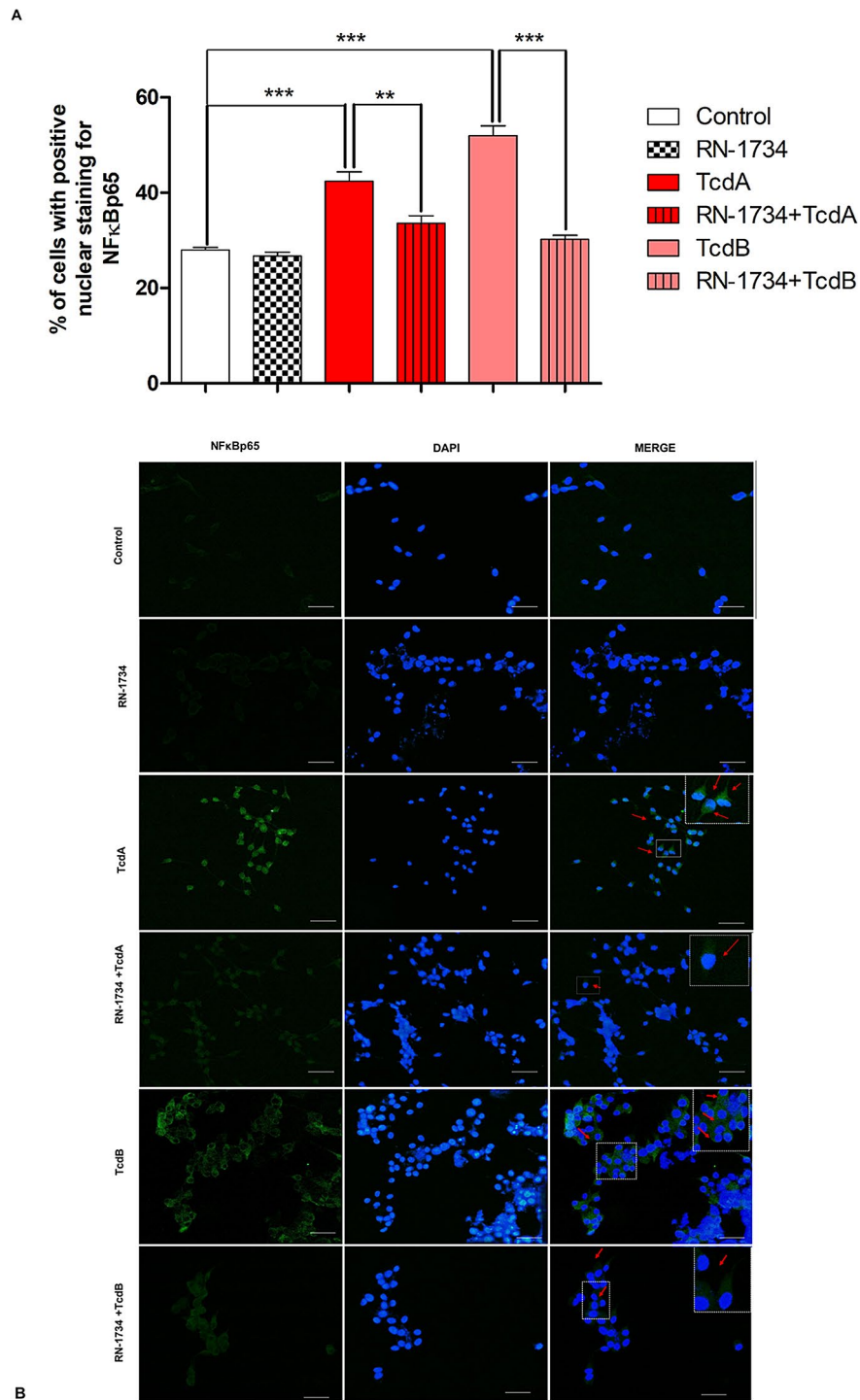


Fig. 4 Blocking TRPV4 with RN-1734 partially prevents the activation of NFκB induced by *C. difficile* toxins **A** (TcdA) and **B** (TcdB) in enteric glial cells (EGCs). **A**) The data represent a quantitative analysis of the percentage of EGCs showing positive nuclear immunostaining for NFκBp65 after 18 h of incubation with either TcdA (50ng/mL), TcdB (1ng/mL), EGCs with only DMEM (control group), RN -1734 alone (100μM), RN-1734 plus TcdA or RN-1734 plus TcdB. TcdA and TcdB activate TRPV4, leading to increased translocation of NFκBp65 to the nuclei of EGCs. Conversely, blocking the receptor with RN-1734 decreases this nuclear translocation compared to the toxin groups. Data are presented as mean ± SEM of the percentage of nuclei with positive immunostaining for NFκBp65. Statistical significance was determined using the one-way ANOVA and Tukey tests. ** $p < 0.001$ and *** $p < 0.0001$. **B**) Photomicrographs illustrate the nuclear immunostaining of NFκBp65 (green), the nuclear staining with DAPI (blue), and the merged images (MERGED). Red arrows indicate the nuclear translocation of NFκB. The percentage of cells positive for NFκBp65 was evaluated in every 100 cells counted ($n = 5$), specifically targeting the hot areas of each group (areas showing intense staining). Scale bars = 50 μm

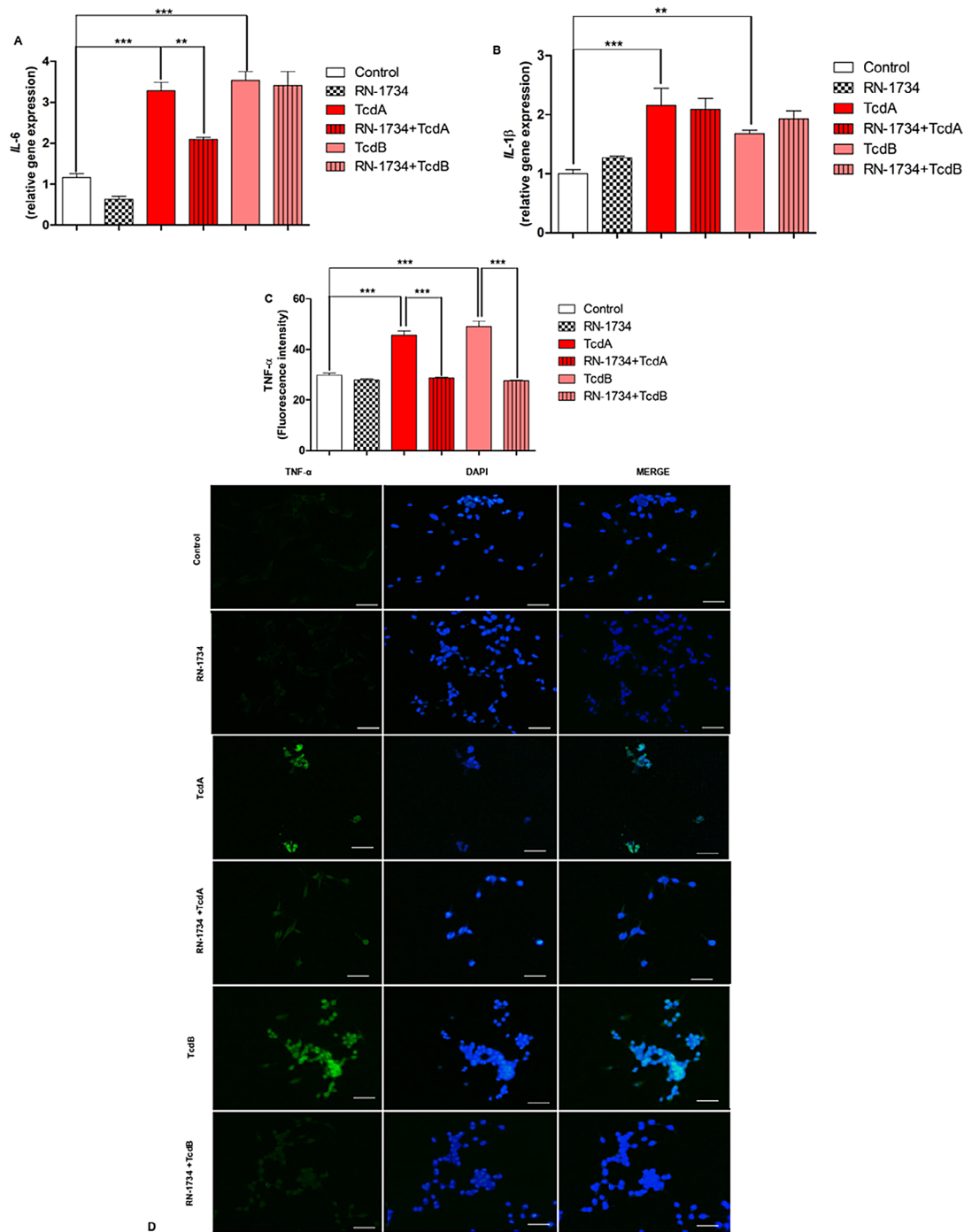


Fig. 5 TRPV4 modulates the inflammatory response of *C. difficile* toxins in enteric glial cells (EGCs). **A**) Inhibition of TRPV4 by the antagonist RN-1734 decreases *IL-6* gene expression in EGCs exposed to TcdA, but not TcdB, over an 18-hour incubation period. *IL-6* gene expression in EGCs was assessed by qPCR. Data are presented as mean ± SEM ($n=6$) of relative *IL-6* gene expression. Statistical significance was determined using the one-way ANOVA and Tukey tests. $**p < 0.001$ and $***p < 0.0001$. **B**) Exposure to TcdA and TcdB increased the *IL-1β* gene expression in EGCs compared to controls. TRPV4 inhibition by RN-1734 does not significantly mitigate the upregulation of *IL-1β* gene expression by TcdA and TcdB. *IL-1β* gene expression in EGCs was assessed by qPCR. Data are presented as mean ± SEM ($n=6$) of relative *IL-1β* gene expression. Statistical significance was determined using the one-way ANOVA and Tukey tests. $**p < 0.001$ and $***p < 0.0001$. **C**) This graph illustrates a quantitative assessment of TNF- α fluorescence in EGCs following 18 h of incubation with either TcdA (50ng/mL), TcdB (1ng/mL), only EGCs with only DMEM (control group), RN -1734 alone (100μM), RN-1734 plus TcdA or RN-1734 plus TcdB. Zeiss software determined the fluorescence intensity in 5 hot areas per slide ($n=6$) (areas showing intense staining). Data are presented as mean ± SEM of TNF- α fluorescence intensity. Statistical significance was determined using the one-way ANOVA and Tukey tests. $***p < 0.0001$. **D**) Representative photomicrographs illustrate TNF- α immunofluorescence (green), the nuclear staining with DAPI (blue), and the merged images (MERGED). Scale bars = 50 μm

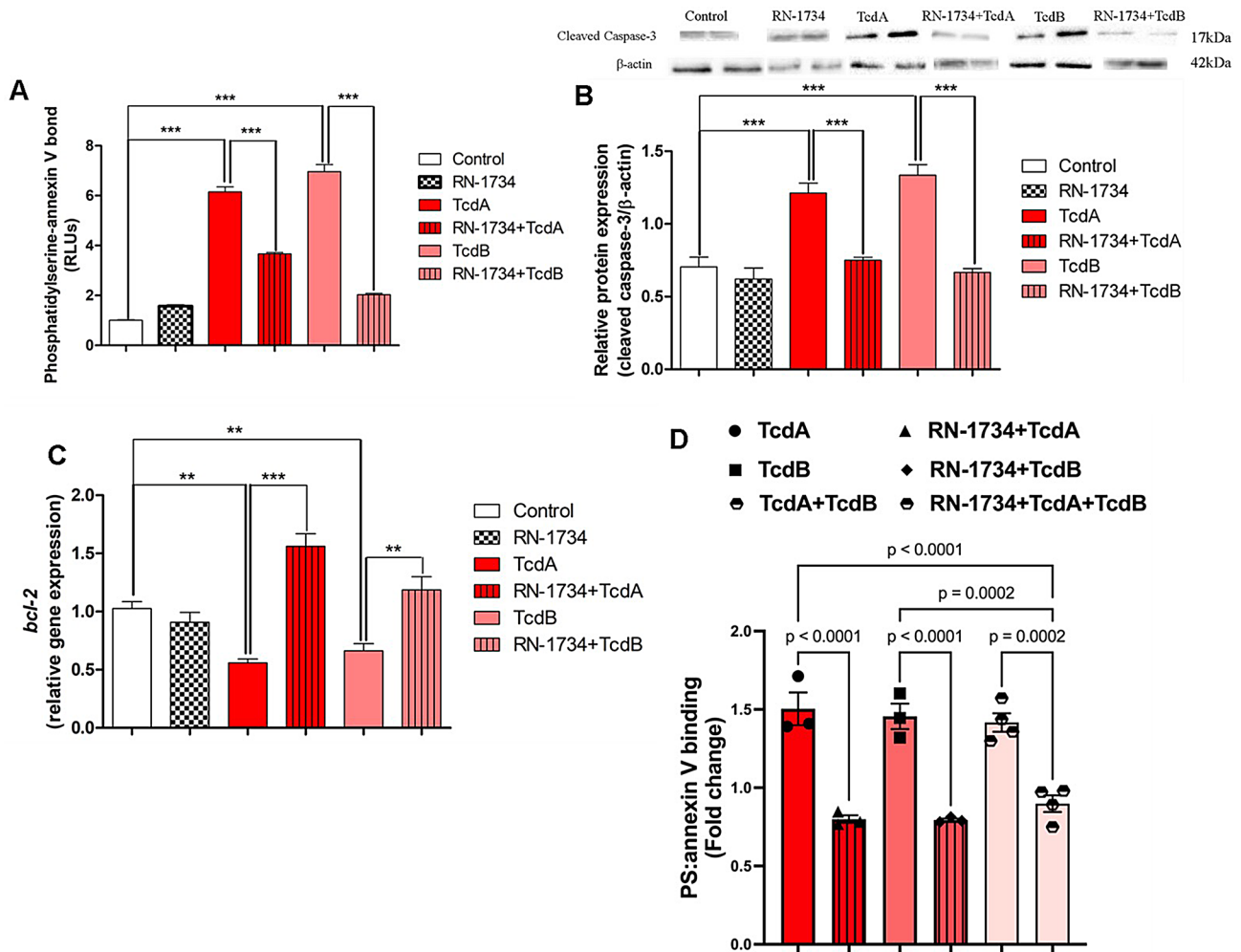


Fig. 6 TRPV4 regulates cell death in enteric glial cells (EGCs) induced by *C. difficile* toxins. **A**) Inhibition of TRPV4 by the antagonist RN-1734 significantly reduced cell death in EGCs exposed to TcdA and TcdB over an 18-hour incubation period. Apoptosis was assessed using the Glo-annexin V real-time assay. Data are presented as mean±SEM ($n=5$) of the relative luminescence units (RLUs), proportional to the amount of phosphatidylserine-annexin V binding. Statistical significance was determined using ANOVA and Tukey tests. $***p < 0.0001$. **B**) Inhibition of TRPV4 by the antagonist RN-1734 significantly reduced the cleaved caspase-3 protein expression in EGCs exposed to TcdA and TcdB over an 18-hour incubation period. Western Blotting detected protein expression in EGCs. Data are presented as mean±SEM ($n=5$) of cleaved Caspase-3 protein expression relative to β-actin. Statistical significance was determined using one-way ANOVA and Tukey tests. $***p < 0.0001$. **C**) Inhibition of TRPV4 by the antagonist RN-1734 significantly upregulates bcl-2 gene expression in EGCs exposed to TcdA and TcdB over an 18-hour incubation period compared to the control group. Gene expression of bcl-2 in EGCs was assessed by qPCR. Data are presented as mean±SEM of relative bcl-2 gene expression. Statistical significance was determined using one-way ANOVA and Tukey tests. $**p < 0.001$ and $***p < 0.0001$. **D**) The inhibition of TRPV4 by the antagonist RN-1734 significantly reduced EGC death following simultaneous exposure to TcdA and TcdB over an 18-hour incubation period. Apoptosis was assessed using the Glo-Annexin V Real-Time Assay, with data presented as mean±SEM ($n=3-5$) of relative luminescence units (RLUs), proportional to phosphatidylserine-annexin V binding. Statistical significance was determined using ANOVA followed by Tukey's post hoc test. EGCs following 18 h of incubation with either TcdA (50ng/mL), TcdB (1ng/mL), only EGCs with only DMEM (control group), RN -1734 alone (100μM), RN-1734 plus TcdA or RN-1734 plus TcdB. The entire blotting membranes are available in the supplementary material (Figure S4–S8)

These findings highlight the role of TRPV4 activation in modulating apoptosis in EGCs, specifically in response to *C. difficile* toxins (See Fig. 7).

TRPV4 antagonist inhibits calcium influx in EGC exposed to *C. difficile* toxins

To further investigate the role of TRPV4 in modulating calcium influx, we measured intracellular calcium levels in enteric glial cells (EGCs) following exposure to *C.*

difficile toxins. Calcium influx was assessed using the Fluo-8 no wash Calcium assay. Cells were challenged with either TcdA (50 ng/mL) or TcdB (1 ng/mL) at multiple time points (0, 3, 4, 6, and 9 h). The results demonstrated a time-dependent increase in calcium levels upon exposure to the toxins (Fig. 8A).

In another experiment, we examined whether blocking TRPV4 with its antagonist, RN-1734, could reduce toxin-induced calcium influx. EGCs were pre-treated with 100

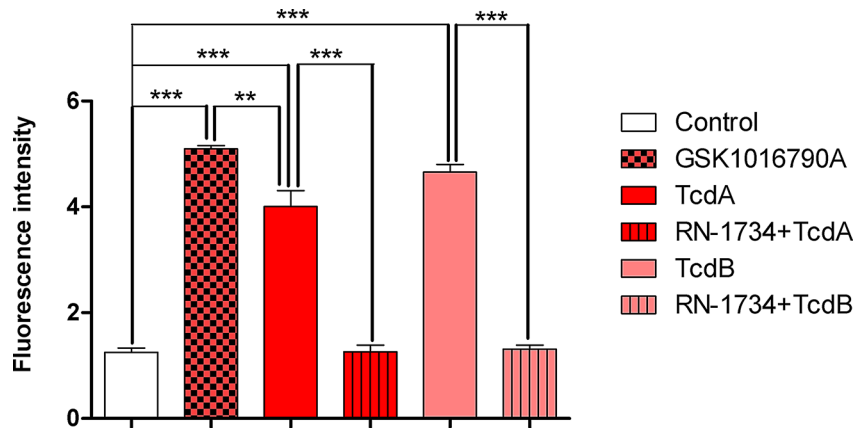


Fig. 7 TRPV4 activation promotes cell death in enteric glial cells (EGCs) via caspase-3 activation, while its inhibition reduces toxin-induced effects. Fluorescence intensity of cleaved caspase-3 was measured in EGCs after 18 h of incubation with GSK1016790A (TRPV4 agonist), TcdA (50 ng/mL), TcdB (1 ng/mL), RN-1734 (TRPV4 antagonist), or their combinations. TRPV4 activation significantly increased caspase-3 cleavage, while its inhibition by RN-1734 reduced the effect induced by both TcdA and TcdB. Data are presented as mean ± SEM (n=5). Statistical significance was determined using one-way ANOVA and Tukey tests. **p < 0.001, ***p < 0.0001. EGCs following 18 h of incubation with either TcdA (50ng/mL), TcdB (1ng/mL), only EGCs with only DMEM (control group), GSK 1,016,790 A (50nM/mL); RN -1734 alone (100µM), RN-1734 plus TcdA or RN-1734 plus TcdB

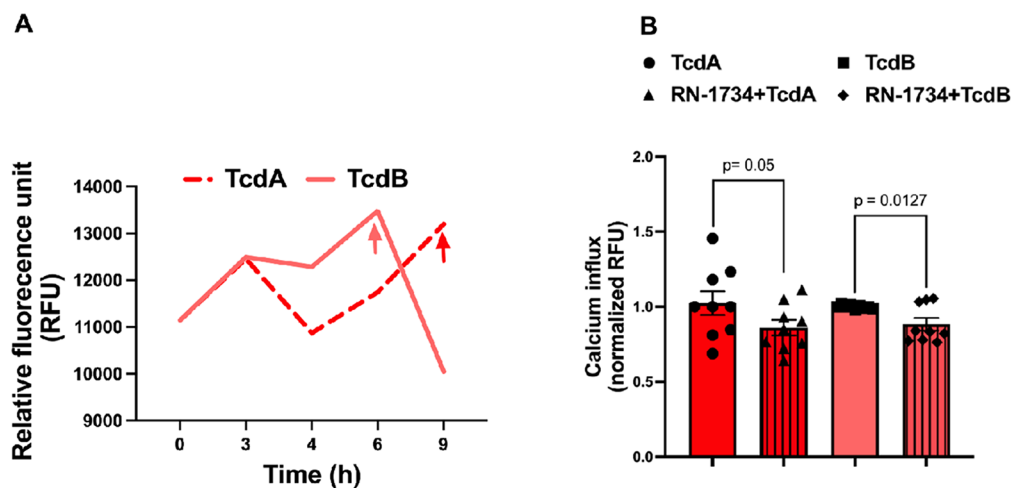


Fig. 8 TRPV4 antagonist reduces calcium influx in enteric glial cells (EGCs) exposed to *C. difficile* toxins. **(A)** Calcium influx was measured using the Fluo-8 No Wash Calcium Assay in EGCs exposed to TcdA (50 ng/mL) or TcdB (1 ng/mL) at various time points (0, 3, 4, 6, and 9 h). **(B)** Calcium influx was measured after 9 h of exposure to TcdA and 6 h of exposure to TcdB in the presence or absence of 100 µM RN-1734 (a TRPV4 antagonist), which was added 1 h prior to toxin exposure. Statistical analysis was performed using Student’s t-test

µM RN-1734 for 1 h before being exposed to TcdA for 9 h or TcdB for 6 h. The TRPV4 antagonist significantly reduced calcium influx in both toxin-treated groups, confirming the involvement of TRPV4 in the calcium regulation pathway triggered by *C. difficile* toxins (Fig. 8B).

Discussion

In this study, we provide new evidence indicating that TRPV4 plays a pivotal role in regulating the inflammatory response and EGCs death triggered by *C. difficile* toxins. Our research illuminates a previously poorly explored area within gastroenterological science, emphasizing the significant impact of *C. difficile* toxins on EGCs. This focus is particularly noteworthy given the extensive

research traditionally dedicated to other gut cell types, such as epithelial cells, while the involvement of EGCs has remained relatively overlooked. By identifying the TRPV4 receptor’s modulation in this context, our study fills a critical gap in our understanding of gut pathology. It opens new avenues for therapeutic interventions targeting gut inflammation and cell death mechanisms.

We observed a marked increase in TRPV4 expression in the cecum and colon of mice infected with *C. difficile*, with a particular concentration in the submucosa, the myenteric plexus, and within enteric immune cells. While the overexpression of TRPV4 in association with CDI is a novel finding, existing literature has documented TRPV4 expression in the myenteric plexus of the colon in mice

experiencing conditions such as visceral hypersensitivity and intestinal dysmotility [16–19]. This observation indicates that TRPV4 may have a role in post-infection dysmotility linked with CDI, a functional disorder documented in the literature [23]. Furthermore, TRPV4 expression has been noted in the myenteric plexus of human colon samples from individuals with IBD such as Crohn's disease and ulcerative colitis [24], highlighting its potential relevance in a broader spectrum of gastrointestinal pathologies.

Expanding on our research, we explored the expression of the TRPV4 receptor in EGCs and discovered that EGCs naturally express the TRPV4 receptor on their cell membranes. Furthermore, we demonstrate that exposure to TcdA and TcdB results in a time-dependent upregulation of this receptor's expression in these cells. Moreover, our research demonstrates that CDI significantly elevates the expression of this receptor in the submucosal and myenteric plexus regions of the cecum and colon in mice.

EGCs are pivotal for many essential physiological functions within the intestine. These include regulating motility, maintaining mucosal integrity, managing secretion, and neurotransmission, and overseeing the regulation of the enteric immune system [25, 26]. Additionally, EGCs are emerging as active components within the ENS, playing crucial roles during intestinal inflammatory and immune responses. The literature has documented a pivotal shift in EGCs, transitioning to a pro-inflammatory phenotype in response to pathological stimuli, such as bacterial products [12, 27]. A pronounced increase in the expression of various receptors and membrane ion channels, including toll-like receptor, P2X receptor, connexin-43, and pannexin-1, marks this transformation [6, 9, 11, 28]. Notably, to our knowledge, the overexpression of TRPV4 in EGCs in response to bacterial products is reported for the first time in the present study.

Moreover, studies in the literature, including those conducted by our group, have demonstrated that EGCs contribute to the inflammatory response by releasing cytokines and glial mediators, such as S100B, GDNF, TNF- α , and IL-1 β [29, 30]. Particularly in CDI, it is well established that *C. difficile* toxins can stimulate various cells, including intestinal epithelial cells, immune cells, and neurons, to release cytokines and chemokines [5]. Our recent research sheds light on the impact of TcdA and TcdB on EGCs [8]. We found that these toxins trigger the activation of NF κ B, resulting in a significant increase in IL-6 gene expression, a cytokine critically involved in the onset and progression of CDI [8]. The current study confirms the activation of NF κ B by these toxins in EGCs, leading to a significant upregulation of IL-6 gene expression and a substantial increase in IL-1 β gene expression in these cells. Interestingly, our findings suggest that TRPV4 appears to be implicated only in the effects of

TcdA on increasing IL-6 gene expression. Blocking this receptor did not affect the IL-6 gene upregulation triggered by TcdB in EGCs, nor did it influence the impact of both toxins on IL-1 β gene expression. This suggests the involvement of alternative mechanisms in mediating these responses.

Moreover, we demonstrate that the inhibition of TRPV4 using its antagonist, RN-1734, reduces the translocation of NF κ Bp65 to the nucleus in EGCs and consequently prevents the overexpression of TNF in these cells. This finding suggests that TcdA and TcdB trigger TNF- α release by activating NF κ B in EGCs, with TRPV4 playing a crucial role in mediating these responses. The translocation of NF κ Bp65 to the nucleus is a vital step for activating this transcription factor, highlighting the essential role of TRPV4 in facilitating NF κ B pathway activation in response to *C. difficile* toxins.

NF κ B is a nuclear transcription factor critical in regulating innate and adaptive immune functions [31]. Once activated, NF κ B regulates the expression of several pro-inflammatory genes, including those that encode cytokines (TNF- α , IL-6, IL-1 β , IL-2, IL-8), chemokines (CXCL-1, CXCL-10, MCP-1), and additionally plays a role in inflammasome regulation [31, 32]. These findings align with our data, which show that the activation of NF κ B by TcdA and TcdB resulted in a significant increase in IL-6 and IL-1 β gene expressions in EGCs, subsequently leading to apoptosis of these cells.

Studies have shown the impact of TcdA and TcdB inducing apoptosis in EGCs and other cells, including enteric neurons, enterocytes, immune cells, and nerve cells [5–10, 33–35]. However, the precise mechanism behind cell death induced by *C. difficile* toxins remains incompletely understood. Our research provides new insights, revealing the crucial involvement of TRPV4 in the death of EGCs triggered by *C. difficile* toxins. Interestingly, simultaneous incubation with TcdA and TcdB did not increase cell death compared to treatments with each toxin alone. One possible explanation for this result is that the mechanisms of cell death induced by TcdA and TcdB may reach a threshold level at the concentrations used, where further increases in toxicity are not observed when both toxins are present together. Alternatively, both toxins may trigger similar apoptotic pathways, which might not necessarily amplify cell death when applied simultaneously at these concentrations.

Additionally, our research offers insights into the molecular mechanisms supporting the protective role of TRPV4 inhibition in safeguarding EGCs against the harmful effects of *C. difficile* toxins. Specifically, we observed that the TRPV4 agonist and toxins *C. difficile* significantly increased caspase activation, a key apoptosis effector, in EGCs. Caspase-3 is critical in mediating the enteric glial cell death induced by TcdA or TcdB

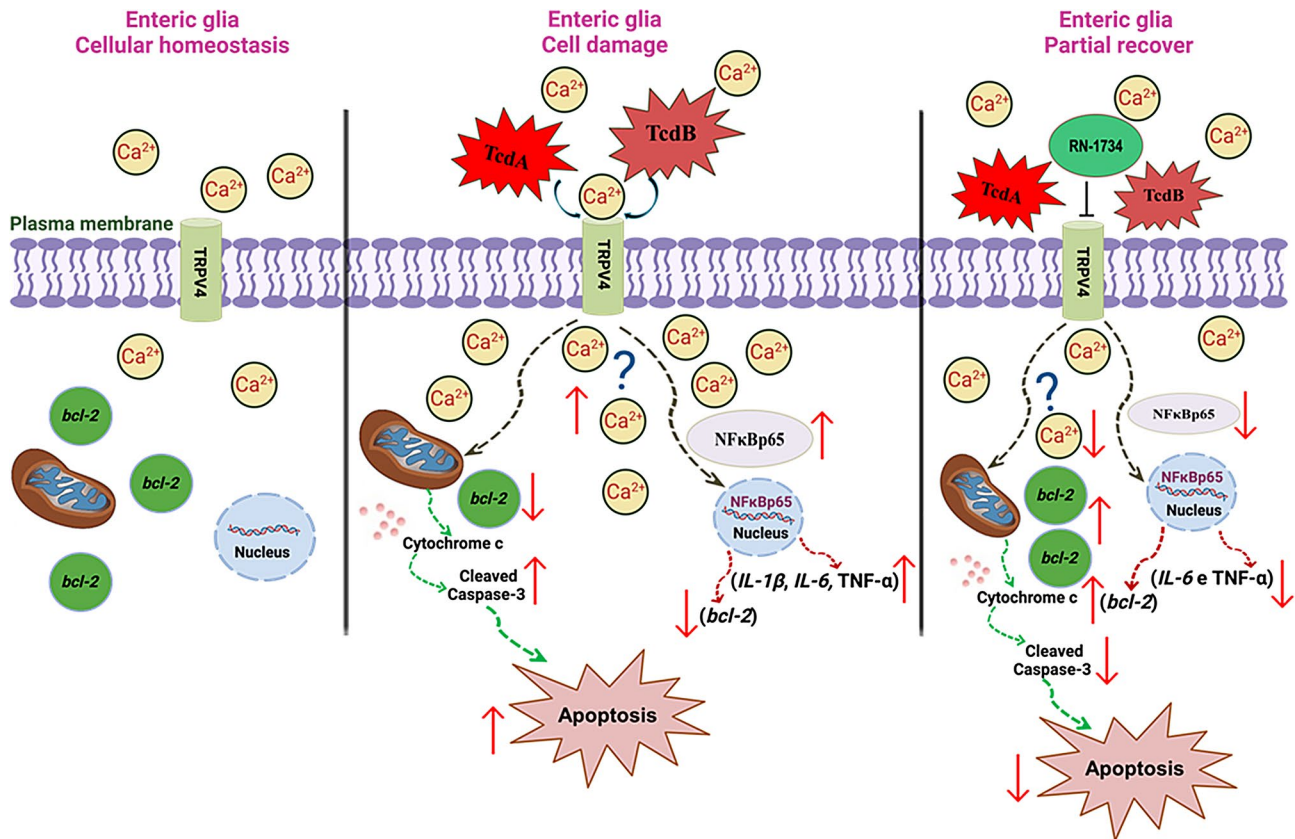


Fig. 9 Possible mechanism of TRPV4 participation in the action of TcdA and TcdB in enteric glia. Cellular homeostasis – enteric glia, under physiological conditions, express the TRPV4 receptor on their cell membranes. Cellular damage – TcdA and TcdB activate the TRPV4 receptor, leading to an increase in its expression and activity in enteric glia and, consequently, triggering a cascade of intracellular events, such as increased translocation of the nuclear transcription factor NFkBp65 to the glial cell nucleus, increased pro-inflammatory cytokines (*IL-6*, *IL-1β* and *TNF-α*), decreased *bcl-2* and increased cleaved caspase-3 which results in the death of enteric glia (apoptosis). These results indicate that toxins increase calcium influx, which affects enteric glia. Partial recovery – Blocking TRPV4 by its antagonist leads to a decrease in the inflammatory response and cell death caused by toxins in glial cells, thus reestablishing the partial physiological conditions of these cells

[9, 36, 37]. The involvement of the TRPV4 receptor in this apoptotic process is further supported by the finding that its inhibition via the antagonist RN-1734 prevented the toxin-induced caspase-3 cleavage. Our study suggests that upon activation by *C. difficile* toxins, TRPV4 increases intracellular Ca²⁺ concentrations, which in turn promotes caspase-3 activation. This was evidenced by the time-dependent increase in calcium levels following toxin exposure. These findings are consistent with previous observations that disruptions in physiological Ca²⁺ levels triggered by TcdA and TcdB are linked to the initiation of cellular death mechanisms [26]. This effect is attributed to the TRPV4 receptor’s notable permeability to Ca²⁺ [38]. Accordingly, blocking TRPV4 significantly reduced calcium influx in both toxin-treated groups, confirming the receptor’s crucial role in the calcium regulation pathway triggered by *C. difficile* toxins.

Furthermore, evidence shows that increased cytoplasmic Ca²⁺ levels can trigger the activation of cell death mechanisms beyond caspases, including pro-apoptotic

members of the B cell lymphoma-2 (Bcl-2) family [5, 33, 36]. The Bcl-2 family of proteins plays a crucial role in regulating apoptosis. This family is categorized into two main sub-groups: the anti-apoptotic proteins that inhibit cell death and the pro-apoptotic proteins that facilitate apoptosis [39]. Our findings demonstrate that TcdA and TcdB reduce the gene expression of the Bcl-2, an anti-apoptotic protein, in EGCs, consequently decreasing cell survival. Significantly, the blockade of the TRPV4 receptor with RN-1734 safeguards the cells against this detrimental effect, suggesting the involvement of this receptor in this specific mechanism.

Another important aspect is that this increase in Ca²⁺ levels may play a crucial role in transforming EGCs into a reactive phenotype. It has been established that EGCs form extensive communication networks through a complex array of Ca²⁺ signals, enabling them to integrate information from neurons, glial cells, immune cells, or other cells in the gut microenvironment [40]. Therefore, the excitability exhibited by EGCs is governed by

their Ca²⁺ responses, highlighting the importance of these signals in potentially driving the transformation of EGCs in response to pathological conditions. The inhibition of TRPV4 might prevent the surge in intracellular Ca²⁺ concentration and its subsequent effects, highlighting a potential therapeutic target in managing the pathological transformation of EGCs.

Our research sheds light on the pivotal role of TRPV4 in mediating the inflammatory response triggered by *C. difficile* toxins and its significant role in the pathogenesis of CDI, marking it as a promising therapeutic target, as illustrated in Fig. 9. However, our study has certain limitations. A more thorough investigation into the impacts of TRPV4 receptor inhibition on CDI outcomes in vivo is essential to fully understand the receptor's activity and implications. Furthermore, the potential clinical application of TRPV4 antagonists requires extensive research to evaluate their effectiveness and safety for human use. These limitations highlight the imperative for ongoing research to deepen our comprehension of TRPV4's role in CDI and to confirm the feasibility of TRPV4-targeted therapies.

Supplementary Information

The online version contains supplementary material available at <https://doi.org/10.1186/s12950-024-00425-7>.

Supplementary Material 1

Acknowledgements

We thank the Center for Studies in Microscopy and Image Processing (NEMPI) of the Department of Morphology at the Federal University of Ceará (UFC) for all the histology services and support for this research. We also thank the creators of BioRender.com, which produced the illustrations in the paper.

Author contributions

All authors contributed to the study's conception and design. DMP, DVSC, MLLB, CSMR, SGS, and MLGSM performed material preparation and data collection. DMP, DVSC, CAW, RFCL, and GACB performed the analysis. DMP, GACB, and RFCL wrote the paper. All authors read and approved the final manuscript.

Funding

The financing project was supported by CNPq from Brazil through grant 408779/2021-7.

Data availability

No datasets were generated or analysed during the current study.

Declarations

Ethics approval

The study's experimental protocol received approval from the Ethics of Animal Experiments Committee at the University of Virginia (Protocol number 4096).

Competing interests

The authors declare no competing interests.

Received: 31 July 2024 / Accepted: 9 December 2024

Published online: 14 January 2025

References

- Zhu D, Sorg JA, Sun X. *Clostridioides difficile* Biology: Sporulation, Germination, and Therapeutic Approaches for *C. difficile* Infection. *Front Cell Infect Microbiol.* 2018;8:29. <https://doi.org/10.3389/fcimb.2018.00029>.
- Mitchell M, Nguyen SV, Macori G, Bolton D, McMullan G, Drudy D, et al. *Clostridioides difficile* Potential Pathogen of Importance to Health. *Healthcare Review.* *Foodborne Pathog Dis.* 2022;19:806–16. <https://doi.org/10.1089/fpd.2022.0037>.
- Pacífico DM, Costa CL, Moura H, Barr JR, Maia GA, Filho VB et al. Exoproteomic analysis of two MLST clade 2 strains of *Clostridioides difficile* from Latin America reveal close similarities. *Sci Rep.* 2021;11: 12373. | <https://doi.org/10.1038/s41598-021-92684-0>
- Bassotti G, Fruganti A, Maconni G, Marconni P, Fettucciari K. *Clostridioides difficile* infection in patients with inflammatory bowel disease may be favoured by the effects of proinflammatory cytokines on the Enteroglial Network. *J Inflamm Res.* 2021;30:7443–53. <https://doi.org/10.2147/JIR.S328628>.
- Fettucciari K, Marguerie F, Fruganti A, Marchegiani A, Spaterna A, Brancorsini S, et al. *Clostridioides difficile* toxin B alone and with pro-inflammatory cytokines induces apoptosis in enteric glial cells by activating three different signaling pathways mediated by caspases, calpains, and cathepsin B. *Cell Mol Life Sci.* 2022;79:442. <https://doi.org/10.1007/s00018-022-04459-z>.
- Santos AQA, Costa DVS, Foschetti DA, Duarte ASG, Martins CS, Soares PMG, et al. P2X7 receptor blockade decreases inflammation, apoptosis, and enteric neuron loss during *Clostridioides difficile* toxin A-induced ileitis in mice. *World J Gastroenterol.* 2022;28:4075–88. <https://doi.org/10.3748/wjg.v28.i30.4075>.
- Ok MT, Liu J, Bliton RJ, Hinesley CM, San Pedro EET, Breau KA et al. A leaky human colon model reveals uncoupled apical/basal cytotoxicity in early *Clostridioides difficile* toxin exposure. *Am J Physiol Gastrointest Liver Physiol* 324(4): G262–80. <https://doi.org/10.1152/ajpgi.00251.2022>
- Costa DVS, Moura-Neto V, Bolick DT, Guerrant RL, Fawad JA, Shin JH, et al. S100b inhibition attenuates intestinal damage and diarrhea severity during *Clostridioides difficile* infection by modulating inflammatory response. *Front Cell Infect Microbiol.* 2021;11:739874. <https://doi.org/10.3389/fcimb.2021.739874>.
- Loureiro AV, Moura-Neto LI, Martins CS, Silva PIM, Lopes MBS, Leitão RFC, et al. Role of Pannexin-1-P2X7R signaling on cell death and pro-inflammatory mediator expression induced by *Clostridioides difficile* toxins in enteric glia. *Front Immunol.* 2022;13:956340. <https://doi.org/10.3389/fimmu.2022.956340>.
- Costa DVS, Shin JH, Goldbeck SM, Bolick DT, Mesquita FS, Loureiro AV, et al. Adenosine receptors differentially mediate enteric glial cell death induced by *Clostridioides difficile* toxins a and B. *Front Immunol.* 2022;13:956326. <https://doi.org/10.3389/fimmu.2022.956326>.
- Seguella L, Gulbransen BD. Enteric glial biology, intercellular signaling and roles in gastrointestinal disease. *Nat Rev Gastroenterol Hepatol.* 2021;18:571–587. <https://doi.org/10.1038/s41575-021-00423-7>.
- López-Gómez L, Szymaszkiwicz A, Zielinska M, Abalo R. Nutraceuticals and enteric glial cells. *Molecules.* 2021;26:3762. <https://doi.org/10.3390/molecules26123762>.
- Liu C, Yang J. Enteric glial cells in immunological disorders of the gut. *Front Cell Neurosci.* 2022;16:895871. <https://doi.org/10.3389/fncel.2022.895871>.
- Nguyen TN, Siddiqui G, Veldhuis NA, Poole DP. Diverse roles of TRPV4 in macrophages: a need for unbiased profiling. *Front Immunol.* 2021;12:828115. <https://doi.org/10.3389/fimmu.2021.828115>.
- Everaets W, Nilius B, Owsianik G. The vanilloid transient receptor potential channel TRPV4: from structure to disease. *Prog Biophys Mol Biol.* 2010;63:2–17. <https://doi.org/10.1016/j.pbiomolbio.2009.10.002>.
- Fichna J, Poole DP, Veldhuis N, MacEachern SJ, Saur D, Zakrzewski PK et al. Transient receptor potential vanilloid 4 inhibits mouse colonic motility by activating NO-dependent enteric neurotransmission. *J Mol Med* 2015;93: 1297–309. <https://doi.org/10.1007/s00109-015-1336-5>
- Yin J, Michalick L, Tang C, Tabuchi A, Goldenberg N, Dan Q, et al. Role of transient receptor potential vanilloid 4 in Neutrophil activation and Acute Lung Injury. *Am J Respir Cell Mol Biol.* 2016;54:370–83. <https://doi.org/10.1165/rcmb.2014-0225OC>.
- Luo J, Qian A, Oetjen LK, Yu W, Yang P, Feng J et al. (2018). TRPV4 Channel Signaling in Macrophages Promotes Gastrointestinal Motility via Direct Effects on Smooth Muscle Cells. *Immunity.* 2016;49: 107–119.e4. <https://doi.org/10.1016/j.immuni.2018.04.021>
- Brierley SM, Page AJ, Hughes PA, Adam B, Liebrechts T, Cooper NJ, et al. Selective role for TRPV4 ion channels in visceral sensory pathways. *Gastroenterology.* 2008;134:2059–69. <https://doi.org/10.1053/j.gastro.2008.01.074>.

20. Chen Y, Mu J, Zhu M, Mukherjee A, Zhang H. Transient receptor potential channels and inflammatory bowel disease. *Front Immunol.* 2020;11:180. <https://doi.org/10.3389/fimmu.2020.00180>.
21. Nogueira LT, Costa DVS, Gomes AS, Martins CS, Silva AMHP, Coelho-Aguar JM, et al. The involvement of mast cells in the irinotecan-induced enteric neurons loss and reactive gliosis. *J Neuroinflammation.* 2017;179. <https://doi.org/10.1186/s12974-017-0854-1>.
22. Ruhl A, Trotter J, Stremmel W. Isolation of enteric glia and establishment of transformed enteroglia cell lines from the myenteric plexus of adult rat. *Neurogastroenterol Motil.* 2001;13:95–106. <https://doi.org/10.1046/j.1365-2982.2001.00246.x>.
23. Gutiérrez RL, Riddle MS, Porter CK. Increased risk of functional gastrointestinal sequelae after *Clostridium difficile* infection among active duty United States military personnel (1998–2010). *Gastroenterology.* 2015;149. <https://doi.org/10.1053/j.gastro.2015.07.059>. 408–14.
24. Wiese JJ, Manna S, Kuhl AA, Fasci A, Elezkurtaj S, Sonnenberg E, et al. Myenteric Plexus Immune Cell Infiltrations and Neurotransmitter Expression in Crohn's Disease and Ulcerative Colitis. *J Crohn's Colitis.* 2024;18(1):121–33. <https://doi.org/10.1093/ecco-jcc/jjad122>.
25. Bassotti G, Marchegiani A, Marconi P, Fettucciarri K. The cytotoxic synergy between *Clostridioides difficile* toxin B and proinflammatory cytokines: an unholy alliance favoring the onset of *Clostridioides difficile* infection and relapses. *Microbiology.* 2020;9:e1061. <https://doi.org/10.1002/mbo3.1061>.
26. Pawolski V, Schmidt MHH. Neuron-Glia Interaction in the developing and adult enteric nervous system. *Cell.* 2021;10:47. <https://doi.org/10.3390/cells1010047>.
27. Progatzy F, Pachnis V. The role of enteric glia in intestinal immunity. *Curr Opin Immunol.* 2022;77:102183. <https://doi.org/10.1016/j.coi.2022.102183>.
28. Esposito G, Capoccia E, Turco F, Palumbo I, Lu J, Steardo A, et al. Palmitoylethanolamide improves colon inflammation through an enteric glia/toll like receptor 4-dependent PPAR- α activation. *Gut.* 2014;63:1300–12. <https://doi.org/10.1136/gutjnl-2013-305005>.
29. Berre CL, Naveilhan P, Rolli-Derkinderen M. Enteric glia at center stage of inflammatory bowel disease. *Neurosci Lett.* 2023;809:137315. <https://doi.org/10.1016/j.neulet.2023.137315>.
30. Costa DVC, Bon-Frauches AC, Silva AMHP, et al. 5-Fluorouracil induces enteric neuron death and glial activation during intestinal mucositis via a S100B-RAGE-NF κ B-Dependent pathway. *Sci Rep.* 2019;24:665. <https://doi.org/10.1038/s41598-018-36878-z>.
31. Liu T, Zhang L, Joo D, Sun SC. NF- κ B signaling in inflammation. *Signal Transduct Target Ther.* 2017;2:17023. <https://doi.org/10.1038/sigtrans.2017.23>.
32. Wolf J, Rose-John S, Garbers C. Interleukin-6 and its receptors: a highly regulated and dynamic system. *Cytokine.* 2014;70:11–20. <https://doi.org/10.1016/j.cyto.2014.05.024>.
33. Brito GAC, Fujji J, Carneiro-Filho BA, Lima AAM, Obrig T, Guerrant R. Mechanism of *Clostridium difficile* Toxin A – Induced apoptosis in T84 cells. *J Infect Dis.* 2002;186:1438–47. <https://doi.org/10.1086/344729>.
34. Modi N, Gulati N, Solomon K, Monaghan T, Robins A, Sewell HF, et al. Differential binding and internalization of *Clostridium difficile* toxin A by human peripheral blood monocytes, neutrophils and lymphocytes. *Scand J Immunol.* 2011;74:264–71. <https://doi.org/10.1111/j.1365-3083.2011.02578.x>.
35. Zhang Y, Li Y, Li H, Chen W, Liu W. *Clostridium difficile* toxin B recombinant protein inhibits tumor growth and induces apoptosis through inhibiting Bcl-2 expression, triggering inflammatory responses and activating C-erbB-2 and Cox-2 expression in breast cancer mouse model. *Biomed Pharmacother.* 2018;101:391–8. <https://doi.org/10.1016/j.biopha.2018.02.045>.
36. Fettucciarri K, Dini F, Marconi P, Bassotti G. Role of the Alteration in Calcium Homeostasis in Cell Death Induced by *Clostridioides Difficile* Toxin A and Toxin B. *Biology.* 2023;10:1117. <https://doi.org/10.3390/biology12081117>.
37. Fettucciarri K, Marconi P, Marchegiani A, Fruganti A, Spaterna A, Bassotti G. Invisible steps for a global enemy: molecular strategies adopted by *Clostridioides difficile*. *Ther Adv Gastroenterol.* 2021;14:175628482110327. <https://doi.org/10.1177/17562848211032797>.
38. Ryskamp DA, Frye AM, Phuong TTT, Yarishkin O, Jo AO, Xu Y, et al. TRPV4 regulates calcium homeostasis, cytoskeletal remodeling, conventional outflow and intraocular pressure in the mammalian eye. *Sci Rep.* 2016;6. <https://doi.org/10.1038/srep30583>.
39. Brentnall M, Rodriguez-Menocal L, Guevara RLD, Cepero E, Boise LH. Caspase-9, caspase-3 and caspase-7 have distinct roles during intrinsic apoptosis. *Bmc Cell Biol.* 2013;14:14–32. <https://doi.org/10.1186/1471-2121-14-32>.
40. Ochoa-Cortes F, Turco F, Linan-Rico A, Soghomonyan S, Whitaker E, Whener S, et al. Enteric glial cells: a New Frontier in Neurogastroenterology and Clinical Target for Inflammatory Bowel diseases. *Inflamm Bowel Dis.* 2016;22:433–49. <https://doi.org/10.1097/MIB.0000000000000667>.

Publisher's note

Springer Nature remains neutral with regard to jurisdictional claims in published maps and institutional affiliations.